Formation mechanism and organizational controlling of ultra-fine-grain copper processed by asymmetrical accumulative rolling-bond and annealing

WANG Jun-li[1, 2], XU Rui-dong[3], WANG Shao-hua[1], QIAN Tian-cai[1], SHI Qing-nan[2]

1. Research Center for Analysis and Measurement, Kunming University of Science and Technology,
Kunming 650093, China;
2. Key Lab of Advanced Materials in Rare and Precious and Non-ferrous Metals of Ministry of Education,
Kunming University of Science and Technology, Kunming 650093, China;
3. Faculty of Metallurgical and Energy Engineering, Kunming University of Science and Technology,
Kunming 650093, China

Abstract: The initial copper with large grain sizes of 60−100 μm was processed by six passes asymmetrical accumulative rolling-bond (AARB) and annealing, the ultra-fine-grained (UFG) copper with grain size of 200 nm was obtained, and the microstructures and properties were studied. The results show that there are large sub-structures and also texture component C for the UFG copper obtained by six passes AARB, possessing high strength and microhardness in company with poor elongation and conductivity. Thereafter, the UFG copper was annealed at 220 °C for 35 min, in which the sub-structures disappear, the grain boundaries are composed of big angle grain boundaries, and the textures are composed of a variety of texture components and parts of twins. Compared with the UFG copper obtained by six passes AARB, the tensile strength and yield strength for the UFG copper obtained by six passes AARB and annealing at 220 °C for 35 min are decreased slightly, the elongation and conductivity are improved obviously.

Key words: ultra-fine-grain copper; asymmetrical accumulative rolling-bond; annealing; formation mechanism; organizational controlling; elongation; conductivity

1 Introduction

Ultra-fine-grained (UFG) copper has caused a extensive attention owning to the excellent performance, which has a very important practical value in the fields of fine processing and plastic micro modeling for materials [1−4]. UFG structure in the material is an effective way for high performance, and the continuous preparation technology is very important [5,6]. At present, there are many methods of severe plastic deformation (SPD) to prepare bulk UFG materials [7−9], but they are very difficult to realize the continuous preparation [10−13]. The preparation of UFG materials such as IF steel, Cu, Al and Al alloy has been succeeded by accumulative rolling-bond (ARB) technology [14], while the preparation process must be carried out under high temperatures in order to eliminate work hardening, raw edges and promote interface combination which decrease the preparation efficiency for UFG materials [15,16]. There are some other reports on asymmetrical rolling (AR) technology for UFG materials [17−19], in which the reduction rate is very large, and sometimes, the maximum reduction rate reaches 99.99%, but the cumulative deformation strain is relatively small because of the limit of the process [20].

Asymmetrical accumulative rolling-bond (AARB) technology has developed from asymmetrical rolling technology and accumulative rolling-bond technology, in which the asymmetrical process can be realized by a pair of rollers with different diameters and UFG materials can be obtained [21]. The introduction of asymmetrical process into ARB technology leads to compressive deformation and shear deformation because of the

existence of shear stresses for the asymmetric, which promotes the interface combination and makes the rolling process conduct at room temperature and accelerates grain refinement. Compared with the conventional preparation method for powder nano-materials, AARB technology can produce bulk UFG materials, in which the processing step from powder materials to bulk materials is omitted, and some shortcomings can also be avoided during the course of preparation [22−25]. In this work, UFG copper with grain size of 200 nm has been obtained by six passes AARB and annealing, the microstructures and properties for the UFG copper are studied, and the formation mechanism and organizational controlling for the UFG copper are discussed.

2 Experimental

The initial copper sheet with grain sizes of 60−100 μm was used in the experiments, and the chemical components are shown in Table1.

Table 1 Chemical compositions for initial copper sheet (mass fraction, %)

Cu	Bi	Sb	Fe	Pb	S	P	O	Others
99.95	0.001	0.002	0.005	0.005	0.005	0.003	0.003	0.026

The initial copper sheet was processed like the rectangular shape with dimensions of 400 mm ×30 mm ×0.8 mm. Six passes AARB was conducted to the initial copper, in which the reduction rate was controlled at 50%, the asymmetry ratio was controlled at 1.08, the equivalent strain was controlled at 4.8, the rolling speed was controlled at 100 r/min, and no lubrication was introduced. The first step was the roughness treated for bonding surfaces. Thereafter, the roughness treated copper was cut in middle, and the roughness treated surfaces were lapped to roll for one pass. Above same process was repeated until the sixth pass and the UFG copper (Deformed copper) was obtained by six passes AARB, the microstructures, microhardness, strength, elongation and conductivity for the UFG copper were tested. Then, the UFG copper obtained by six passes AARB was annealed at 220 °C for 20 min and 35 min, respectively, the microstructures and component textures for the UFG copper were observed, and the microhardness, strength, elongation and conductivity were also tested.

XL30[TMP] SEM+EBSD and Dmax/2200 XRD texture accessory were used to measure the microstructures and texture components for UFG copper. During the course of XRD measurement, the voltage of ray tube was 30 kV, the current of ray tube was 50 mA, divergence slit was 1.2 mm×3 mm, receiving slit was 3

mm and the monochromator was used. TEM was used to measure the microstructures for UFG copper. HX−1 microhardness tester was used to measure the microhardness for the initial copper and UFG copper. AG−250KNE tensile tester was used to measure the strength and elongation for the initial copper and UFG copper, and the sizes for the tested samples were processed according to GB/T228−2002 standards. 7501 Eddy current conductivity meter was used to measure the conductivity for the initial copper and the UFG copper.

3 Results and discussion

3.1 Microstructures and properties for UFG copper obtained by six passes AARB

Microstructure and texture for UFG copper obtained by six passes AARB are shown in Fig. 1. Figure 1(a) shows the TEM photograph of rolling plane for the UFG copper, it can be seen that the grain sizes for the UFG copper are refined and reach 200 nm in the order of UFG magnitude. Simultaneously, some dislocation webs form and several small sub-grains generate in parts of refined grains. Figure 1(b) shows the {111} pole figure of the rolling plan for the UFG copper obtained by six passes AARB, which exhibits that {112}<111> is the main
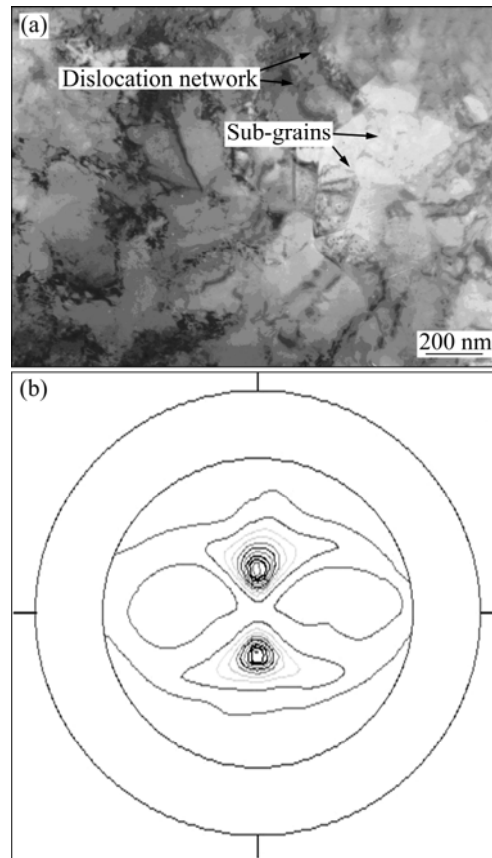
Fig. 1 Microstructure and texture for UFG copper obtained by six passes AARB with TEM photograph of rolling plane (a) and (111) pole figure of rolling plan, examined by XRD (b)

texture component, which is a typical texture component C. So, the UFG copper obtained by six passes AARB is the deformed copper.

The properties for the UFG copper obtained by six passes AARB are listed in Table 2. It is obvious that the microhardness is HV110.7, the tensile strength is 455.7 MPa, the yield strength is 349.6 MPa, the elongation is 2.1%, and the conductivity is 45.4 MS/m. Therefore, compared with the initial copper, the tensile strength, yield strength and microhardness for the UFG copper obtained by six passes AARB are improved obviously, while the elongation and conductivity are decreased obviously. Figure 1 shows that there have many structure defects, sub-structures and obvious preferred orientations in the UFG copper obtained by six passes AARB, which leads to the increase of the microhardness and strength in company with the decrease of the elongation and conductivity. Therefore, the UFG copper obtained by six passes AARB needs to be annealed in order to improve the elongation and conductivity further.

3.2 Microstructures and properties for UFG copper obtained by six passes AARB and annealing

To explore annealing technique for the UFG copper obtained by six passes AARB, the annealing experiments were conducted at low temperatures for long time or high temperature for short time, in which the annealing temperatures were controlled in the range from 100 °C to 400 °C. Finally, the determined annealing temperature was controlled at 220 °C.

TEM morphologies for the UFG copper obtained by six passes AARB and annealing at 220 °C for 20 min and 35 min, are shown in Fig. 2. It can be seen in Fig. 2 that a large number of dislocations aggregate towards grain boundaries or other local regions and react with parts of sub-grain boundaries, which leads that some sub-grain boundaries and dislocation tangles disappear when the annealing time is controlled at 20 min. The recovery course for the deformed copper will take place with further increasing the annealing time. Longer annealing time will bring about the nucleation and growth for parts of sub-grains owing to the migration, rotation and aggregation for two or more sub-grain boundaries. When the annealing time is increased to 35 min, there are no defects between grains or in the grains, the microstructures are composed of equiaxed crystals and the grain sizes are still about 200 nm. In the meantime, some twins also appear in the microstructures for the UFG copper.
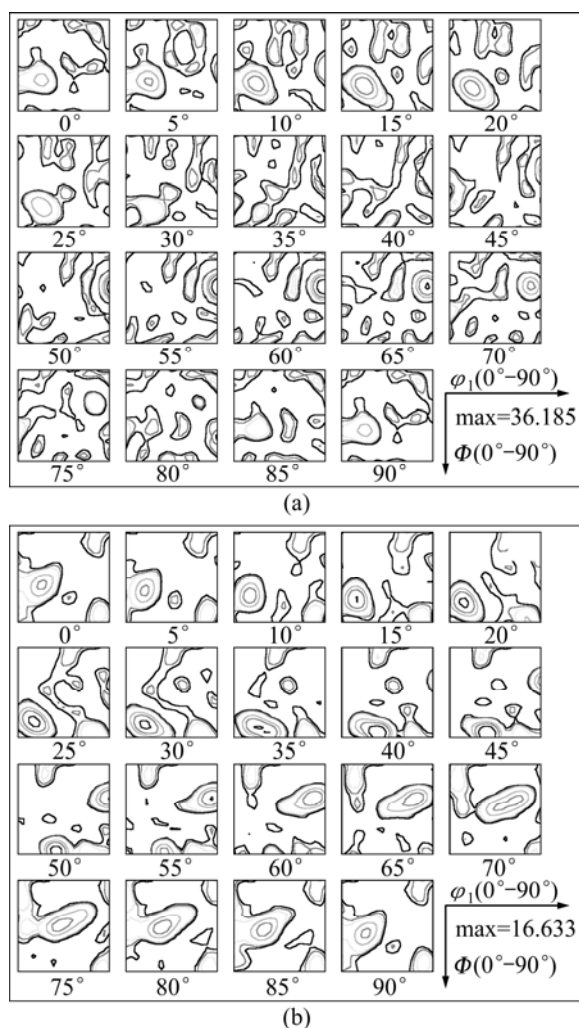
The constant $\varphi2$ sections of orientation distribution function (ODF) for the UFG copper obtained by six passes AARB and annealing at 220 °C for 20 min and 35 min are shown in Fig. 3. Figure 3(a) shows that when the annealing time is controlled at 20 min, the cold-rolling texture component C is reduced further and there have no changes for texture components S and R. At this time, faint B/G components appear and no cube texture components. It can be seen in Fig. 3(b) that when the annealing time is increased to 35 min, the recovery course has finished, the textures are composed of faint

Table 2 Properties of copper for different stages

Processing condition	Microhardness (HV)	Tensile strength, σ_b/MPa	Yield strength, $\sigma_{0.2}$/MPa	Elongation/%	Conductivity/ (MS·m^{-1})
Initial copper	63.0	231.3	101.5	44.0	76.3
UFG copper obtained by six passes AARB	110.7	455.7	349.6	2.1	45.4
UFG copper obtained by six passes AARB and annealing at 220 °C for 20 min	117.9	433.4	320.9	4.6	62.5
UFG copper obtained by six passes AARB and annealing at 220 °C for 35 min	108.8	420.8	318.8	7.2	69.0
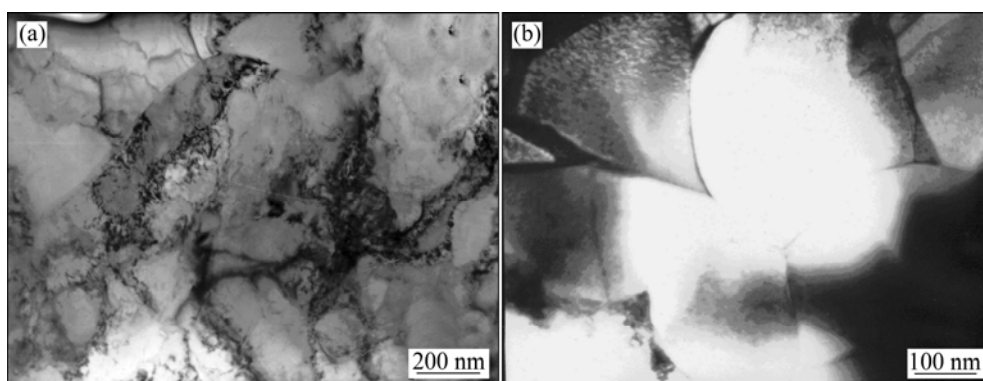
Fig. 2 TEM morphologies for UFG copper obtained by six passes AARB and annealing at 220 °C for 20 min (a) and 35 min (b)

Fig. 3 Constant $\varphi2$ sections of ODF for UFG copper obtained by six passes AARB and annealing at 220 °C for 20 min (a) and 35 min (b) ($\Delta\varphi2=5°$)

cube texture components, other texture components such as R, S, B/G and cold rolled texture components such as B and C, but their strengths are all weak and stable, and the highest texture strength is only 16.6 grades.

The properties of the UFG copper obtained by six passes AARB and annealing at 220 °C for 20 min and 35 min, are also listed in Table 2. As shown in Table 2, when the annealing time is controlled at 20 min and 35 min, the microhardnesses for the UFG copper are HV117.9 and HV108.8, respectively, the tensile strengths are 433.4 MPa and 420.8 MPa, respectively. The yield strengths are 320.9 MPa and 318.8 MPa, respectively, the elongations are 4.6% and 7.2% respectively and the conductivities are 62.5 MS/m and 69.0 MS/m, respectively. Therefore, compared with the initial copper, the tensile strength, yield strength and microhardness for the UFG copper obtained by six passes AARB and annealing at 220 °C for 20 min and 35 min are improved, the elongation is decreased and the conductivity is also

decreased slightly. Compared with the UFG copper obtained by six passes AARB, the tensile strength and yield strength for the UFG copper obtained by six passes AARB and annealing at 220 °C for 20 min and 35 min are decreased slightly, the microhardness change is not obvious, but the elongation and conductivity are improved obviously.

The study on the boundaries is very important because there are a large number of sub-boundaries in the UFG copper. Generally, the grain boundary is divided into high angle grain boundary in which the misorientation is larger than 15°, and the small angle grain boundary in which the misorientation is between 1° and 10° according to the grain misorientation. The grain boundary for the misorientation between 10° and 15° may be defined as the big angle grain boundary or the small angle grain boundary for the research needs. The boundary structure is determined by its characteristics, including relative grain orientation, coincidence site lattice (CSL) and space orientation for grain boundary, etc. The structure for the grain boundary is very complex, thus it is not easy to forecast its microstructures and properties with regard to the boundary with random orientation. Grain boundary misorientation is related to the texture which is the misorientation distribution function for polycrystalline materials. In general, grain boundary with small angle and grain boundary with low value of CSL (≤3) do not rupture and the crackles can make a detour round the grain boundary. There are a large number of grain boundaries with small angle and grain boundaries with a low value of CSL because of the existing of textures in the UFG copper obtained by six passes AARB and annealing at 220 °C for 20 min, which makes grain slipping difficult and leads to low superplasticity or no superplasticity, high creep strength, fracture toughness and oxidation resistance for the UFG copper. The texture characteristics during the course of annealing can be observed by the misorientation analysis, which can display the change of grain boundary for the UFG copper, and can also determine the performance difference for the UFG copper with different grain boundaries.

Misorientation distributions of the UFG copper obtained by six passes AARB and annealing at 220 °C for 20 min and 35 min, are shown in Fig. 4. There are a large number of sub-grains and small angle grain boundaries for the UFG copper obtained by six passes AARB. It can be seen in Fig. 4(a) that when the annealing time is controlled at 20 min (primary annealing course), the grain misorientation is small and no rule, and the different angle misorientations all exist in the UFG copper, therefore, the above course is in the stage of recovery annealing for the deformed copper. As shown in Fig. 4(b), there are no substructures in the UFG

copper when the annealing time is increased to 35 min, most grain misorientation values are high, displaying that the small angle grain boundary has turned to high angle grain boundary, which is consistent with the analysis for the grain boundary during the course of recrystallization. Therefore, it can be seen that the grains are small grains with high angle grain boundaries, and not subgrains for the UFG copper obtained by six passes AARB and annealing at 220 °C for 35 min.
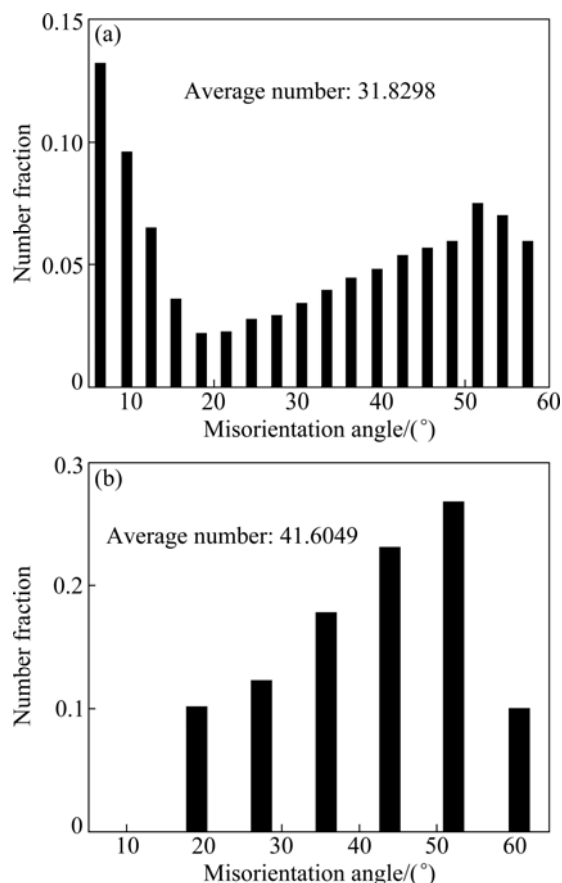
Fig. 4 Misorientation distributions for copper obtained by six passes AARB and annealing at 220 °C for 20 min (a) and 35 min (b)

It can be concluded that the rolling texture characteristics are maintained in the stage of primary annealing, displaying that the recovery or in situ recrystallization happens in the deformed copper. Actually, there is no strict boundary for the recovery and in situ recrystallization because two processes are overlapped to a certain extent. Increasing the annealing time will reduce the strength for the rolling textures in company with the formation and growth of sub-grains, in which the stage still belongs to recovery or continuous recrystallization. Then, an extension of the annealing time will bring out faint cube texture components, other texture components such as R, S, B/G and cube texture components. These are different from typical rolling texture components, displaying that discontinuous

recrystallization happens. A further duration of the annealing time leads to no obvious change of the strengths for texture components during the course of discontinuous recrystallization, showing that the structures for the UFG copper are very stable. Therefore, the sub-structures in the UFG copper obtained by six passes AARB disappear, and the rolling textures disappear or weaken when annealed at 220 °C for 35 min. At this time, the elongation increases greatly with a bit of reduction in the strength for the UFG copper obtained by six passes AARB and annealing at 220 °C for 35 min.

3.3 Formation mechanism and organizational controlling for UFG copper obtained by six passes AARB and annealing

It can be seen from microstructures observation, texture analysis and performance tests that there are a large number of sub-structures and processing textures in the UFG copper obtained by six passes AARB, which brings out working-hardening effects, increases the microhardness, tensile strength and yield strength for the UFG copper and decreases the elongation. In the meantime, the electron motion is hindered which leads to the decline for the conductivity owing to the existence of sub-structures for the UFG copper obtained by six passes AARB.

The microstructures for the UFG copper obtained by six passes AARB can be changed and the sub-structures can be eliminated by annealing, in which the texture components transform from cold-rolling texture component C to texture multicomponents. Therefore, the uniformity for the UFG copper is improved and the grain sizes reach the order of UFG magnitude. It can be concluded that a large of sub-structures combine and react to form a large of grain boundaries for the UFG copper obtained by six passes AARB during the course of annealing, leading to the grain refinement. Theoretically, the increase of grain boundaries caused by the grain refinement will hinder the electron motion and decrease the conductivity of the UFG copper. Factually, the conductivity of the UFG copper is not decreased slightly, the main reasons are that there are some twins in the UFG copper obtained by six passes AARB and annealing at 220 °C for 35 min (see Fig. 5). The boundary energy of twins is lower than that of normal grain boundary, which is faint to the electron inhibition. The increase of grain boundaries caused by the grain refinement and the occurrence of twins cancel out for the movement of electrons [26]. Therefore, the conductivity for the UFG copper obtained by six passes AARB and annealing at 220 °C for 35 min, is declined slightly and almost maintains the level of the initial copper.

Tensile fracture morphologies for the UFG copper

obtained by six passes AARB and annealing at 220 °C for 20 min and 35 min, are shown in Fig. 6. It can be seen in Fig. 6 that there is no obvious necking in the tensile fracture location. Figure 6(a) shows that when the annealing time is controlled at 20 min, the cleavage step and tearing ridge can be observed for the UFG copper in the tensile fracture location, which is a typical brittle fracture feature. It can be seen from Fig. 6(b) that when the annealing time is increased to 35 min, the tensile fracture surface of the UFG copper is the same as Fig. 6(a), but there are other small dimples, which is a mixed fracture feature, displaying that the plastic fracture proportion of the UFG copper obtained by six passes AARB and annealing at 220 °C for 35 min increases and the plasticity increases.
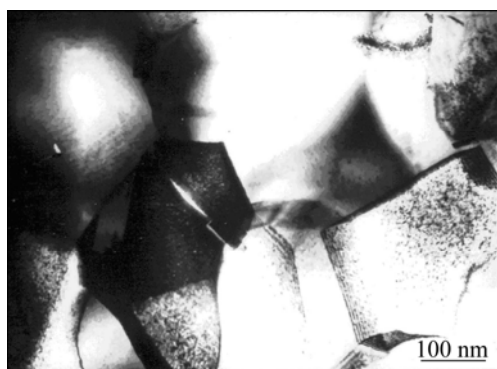
Fig. 5 Twins morphology of UFG copper obtained by six passes AARB and annealing at 220 °C for 35 min
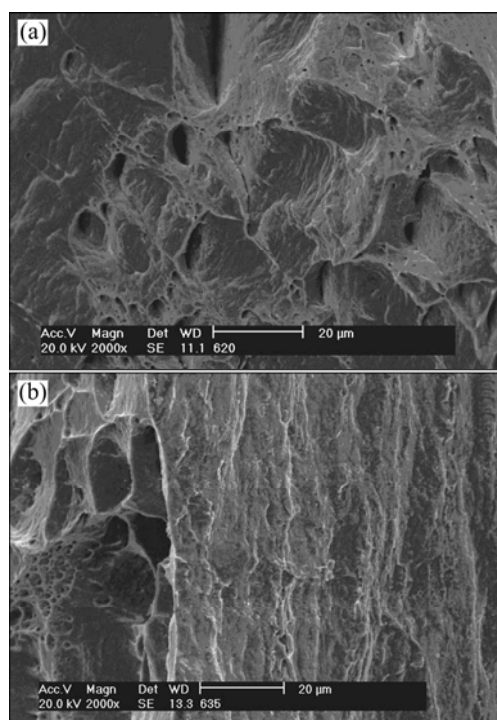
Fig. 6 Tensile fracture morphologies of UFG copper obtained by six passes AARB and annealing at 220 °C for 20 min (a) and 35 min (b)

4 Conclusions

1) UFG copper with grain size of 200 nm obtained by six passes AARB and annealing at 220 °C for 35 min, possesses excellent tensile and yield strength, conductivity and microhardness.

2) There are a large number of sub-structures such as dislocation tangles and sub-grains, and also rolling texture component C exists in the UFG copper (deformed copper) obtained by six passes AARB. Compared with the initial copper, the tensile strength, yield strength and microhardness of the UFG copper are improved obviously in company with the decrease of the elongation and conductivity.

3) The sub-structures disappear for the UFG copper obtained by six passes AARB and annealing at 220 °C for 35 min, in which the grain boundaries are high angle grain boundaries and parts of twins appear. The textures are composed of faint cube texture components and other texture components such as R, S, B/G and cold-rolling texture component C. Compared with the initial copper, the tensile strength, yield strength and microhardness of the UFG copper are improved, the elongation is decreased and the conductivity is decreased slightly. Compared with the UFG copper obtained by six passes AARB, the tensile strength and yield strength are decreased slightly, the microhardness change is not obvious, but the elongation and conductivity are improved obviously.

References

[1]   MISHRA A, MARTIN M, THADHANI N N, KAD B K, KENIK E A, MEYERS A. High-strain-rate response of ultra-fine-grained copper [J]. Acta Materialia, 2008, 56(12): 2770−2783.

[2]   ZHU Yun-tian, LIAO Xiao-zhou. Nanostructured metals retaining ductility [J]. Nature Materials, 2004(3): 351−352.

[3]   HAOUAOUI M, KARAMAN I, MAIER H J. Flow stress anisotropy and Bauschinger effect in ultrafine grained copper [J]. Acta Materialia, 2006, 54(20): 5477−5488.

[4]   WANG H L, WANG Z B, LU K. Interfacial diffusion in a nanostructured Cu produced by means of dynamic plastic deformation [J]. Acta Materialia, 2011, 59(4): 1818−1828.

[5]   PANIGRAHI S K, JAYAGANTHAN R, PANCHOLI V. Effect of plastic deformation conditions on microstructural characteristics and mechanical properties of Al 6063 alloy [J]. Materials and Design, 2009, 30(6): 1894−1901.

[6]   KIM W J, JEONG H G, JEONG H T. Achieving high strength and high ductility in magnesium alloys using severe plastic deformation combined with low-temperature aging [J]. Scripta Materialia, 2009, 61(11): 1040−1043.

[7]   ZHANG Xin-ming, ZHENG Da-wei, YE Ling-ying, TANG Jian-guo. Superplastic deformation behavior and mechanism of 1420 Al−Li alloy sheets with elongated grains [J]. Journal of Central South University of Technology, 2010, 17(4): 659−665.

[8]   TSUJI N, SAITO Y, LEE S H. ARB and other new techniques to produce bulk ultrafine grained materials [J]. Advanced Engineering

Materials, 2003, 5(5): 338−344.

[9]   NAEINI M F, SHARIAT M H, EIZADJOU M. On the chloride-induced pitting of ultra fine grains 5052 aluminum alloy produced by accumulative roll bonding process [J]. Journal of Alloys and Compounds, 2011, 509(14): 4696−4700.

[10] YOON S C, HONG S J, HONG S I, KIM H S. Mechanical properties of equal channel angular pressed powder extrudates of a rapidly solidified hypereutectic Al−20 wt% Si alloy [J]. Materials Science and Engineering A, 2007, 449−451: 966−970.

[11] AZUSHIMA A, KOPP R, KORHONEN A, YANG D Y, MICARI F, LAHOTI G D, GROCHE P, YANAGIMOTO J, TSUJI N, ROSOCHOWSKI A, YANAGIDA A. Severe plastic deformation (SPD) processes for metals [J]. CIRP Annals−Manufacturing Technology, 2008, 57: 716−735.

[12] BEYERLEIN I J, TÓTH L S. Texture evolution in equal-channel angular extrusion [J]. Progress in Materials Science, 2009, 54 (4): 427−510.

[13] ITO Y, HORITA Z. Microstructural evolution in pure aluminum processed by high-pressure torsion [J]. Materials Science and Engineering A, 2009, 503(1−2): 32−36.

[14] TSUJI N, SAITO Y, LEE S H, MINAMINO Y. ARB (Accumulative Roll-Bonding) and other new techniques to produce bulk ultrafine grained materials [J]. Advanced Engineering Materials, 2003, 5(5): 338−344.

[15] SUN Feng-wei，LI Sai-yi. Effect of stacking number in accumulative roll-bonding of commercial-purity aluminum sheets [J]. Light Alloy Fabrication Technology, 2010, 38(2): 33−36. (in Chinese)

[16] ZHANG Bing, YUAN Shou-qian, WEI Ying-juan, ZHANG Xi-feng, LV Shuang. Evolvement of microstructure & properties for 1060 Al during accumulative roll bonding process [J]. Materials for Mechanical Engineering, 2008, 32(1): 67−72. (in Chinese)

[17] HUANG Tao, QU Jia-hui, HU Zhuo-chao, WANG Fu, ZUO Liang. Evolution of the orientation of cross shear rolling high purity aluminum foils during deformation and recrystallization [J]. Acta Metallurgica Sinica, 2005, 41(9): 953−957. (in Chinese)

[18] ZHU Li-da, ZHU Chun-xia, YU Tian-bao, WANG Wan-shan. Study on simulation and experiment of dynamic characteristics of the linear rolling guide in turn-milling centre [J]. Advanced Science Letters, 2011, 4: 1913−1917.

[19] KIM W J, LEE J B, KIM W Y, JEONG H T, JEONG H G. Microstructure and mechanical properties of Mg−Al−Zn alloy sheets severely deformed by asymmetrical rolling [J]. Scripta Materials, 2007, 56(4): 309−312.

[20] SUN Ji-quan, DAI Hui, TANG Di. Development survey and its application prospect of asynchronous rolling technology [J]. Angang Technology, 2009, 359(5): 1−6. (in Chinese)

[21] WANG Jun-li, SHI Qing-nan, QIAN Tian-cai, WANG Shao-hua, YANG Xi-kun. Recrystallized microstructural evolution of UFG copper prepared by AARB process [J]. Transactions of Nonferrous Metals Society of China, 2010, 20 (4): 559−563.

[22] JAHEDI M, PAYDAR M H. Study on the feasibility of the torsion extrusion (TE) process as a severe plastic deformation method for consolidation of Al powder [J]. Materials Science and Engineering A, 2010, 527(20): 5273−5279.

[23] FILHO W J B, FOGAGNOLO J B, RODRIGUES C A D, KIMINAMI C S, BOLFARINI C, YAVARI A R. Consolidation of partially amorphous aluminum alloy powders by severe plastic deformation [J]. Materials Science and Engineering A, 2004, 375−377: 936−941.

[24] KOLOBOV Y R, KIEBACK B, IVANOV K V, WEISSGAERBER T, GIRSOVA N V, POCHIVALOV Y I, GRABOVETSKAYA G P, IVANOV M B, KAZYHANOV V U, ALEXANDROV I V. The structure and microhardness evolution in submicrocrystalline molybdenum processed by severe plastic deformation followed by annealing [J]. International Journal of Refractory Metals and Hard Materials, 2003, 21(1−2): 69−73.

[25] ALEXANDROV I V, ZHU Y T, LOWE T C, ISLAMGALIEV R K, VALIEV R Z. Consolidation of nanometer sized powders using severe plastic torsional straining [J]. Nanostructured Materials, 1998, 10(1): 45−54.

[26] LU L, SHEN Y F, CHEN X H, QIAN L H, LU K. Ultra high strength and high electrical conductivity in copper [J]. Science, 2004, 304(5669): 422-426.

异步叠轧辅助退火制备超细晶铜材的形成机制及组织控制

王军丽[1,2]，徐瑞东[3]，王绍华[1]，钱天才[1]，史庆南[2]

1. 昆明理工大学 分析测试研究中心，昆明 650093；

2. 昆明理工大学 稀贵及有色金属先进材料教育部重点实验室，昆明 650093；

3. 昆明理工大学 冶金与能源工程学院，昆明 650093

摘　要：对原始晶粒大小为 60~100 μm 的铜材进行六道次大变形异步叠轧并辅助退火处理，获得晶粒大小为 200 nm 的超细晶铜材，研究超细晶铜材的微观组织结构和性能。结果表明：六道次大变形异步叠轧后的超细晶铜材组织中存在大量的亚结构，也存在特定织构 C 组分，其强度和显微硬度高但伸长率和电导性下降。经 220 °C、35 min 退火处理后，亚结构消失，晶界由大角度晶界组成，织构由多种织构组分组成，也出现部分孪晶。与六道次大变形异步叠轧的超细晶铜材相比，经 220 °C、35 min 退火处理的超细晶铜材的抗拉强度和屈服强度略有下降，但伸长率和导电性明显提高。

关键词：超细晶铜材；异步叠轧；退火；形成机制；组织控制；伸长率；导电性

(Edited by LI Xiang-qun)